Undersea Biomedical Research, Vol. 3, No. 3, September 1976

Scanning electron microscopy of normoxic and hyperoxic hyperbaric exposed lungs

B.K. ROSS and T.K. AKERS

Department of Physiology and Pharmacology, School of Medicine, University of North Dakota, Grand Forks, ND 58202

Ross, B.K., and T.K. Akers. 1976. Scanning electron microscopy of normoxic and hyperoxic hyperbaric exposed lungs. Undersea Biomed. Res. 3(3):283–299.—Lungs from adult guinea pigs exposed to 1 ATA He–O_2 with 200 mm Hg P_{O_2} and 20 ATA He–O_2 with 200, 400, and 600 mm Hg P_{O_2} were studied with scanning electron microscopy. The appearance of normal alveoli is described. Even before pulmonary O_2 toxicity became symptomatic, subtle changes occurred in the alveoli, such as an increase in macrophages and a marked increase in length of alveolar type-II cell microvilli. These changes occurred in animals exposed to 400 mm Hg P_{O_2}, heretofore considered below toxic levels. With increased toxic involvement, the number of alveolar type-II cells increased. A thick layer of material appeared in some of the alveoli, obscuring the Kohns pores and type-I and -II cell surfaces. The alveolar-capillary network with underlying erythrocytes was no longer observable. Lungs with the greatest toxic involvement possessed large numbers of macrophages encompassed by a fibrin-like matrix. The alveolar walls were broken down in many instances, and the alveoli were no longer discrete units but took on the appearance of an amorphous mass of lung tissue.

oxygen toxicity
alveolus
macrophage
alveolar type-II cells

The internal ultrastructural morphological alterations of pulmonary tissue resulting from various degrees of O_2 toxicity have been carefully studied (Clark and Lambertsen 1971; Adamson, Bowden, and Wyatt 1970; Kapanci, Weibel, Kaplan, and Robinson 1969; Cedergren, Gyllensten, and Wersall 1959; Kistler, Caldwell, and Weibel 1967). Relatively little is known about the alterations in surface morphology of lung alveoli with the development of pulmonary O_2 toxicity, although the alveolar-surface topography plays a vital role in the functional capabilities of the lung. The limitations imposed by the extremely small specimen size for transmission electron microscopy prohibit examination of alveolar-surface characteristics in detail. However, the extremely large depth of field, wide range of magnifications, and relatively high resolving power make the scanning electron microscope (S.E.M.) a powerful tool to permit three-dimensional appreciation of lung structure (Kuhn and Finke 1972).

The first application of S.E.M. to the lung was by Jaques, Coalson, and Zervins in 1965. Since that time there have been a number of S.E.M. studies on the lung and respiratory system (Nowell and Tyler 1971; Kuhn and Finke 1972; Wang and Thurlbeck 1970; Greenwood and Holland 1972) and a number that have dealt with the study of pulmonary pathologies (Holma

1969; Aranyi 1972; Greenwood and Holland 1973). However, as of this writing, few—if any—have applied the techniques of S.E.M. to the study of pulmonary O_2 toxicity. The present study applied S.E.M. in the examination of both normal and O_2 toxic lung tissue to determine the surface morphological characteristics of each.

METHODS

Four groups of 24 adult male guinea pigs (240–400 g) were used in this study. Three groups were continuously exposed to 20-ATA pressure with 200, 400, and 600 mm Hg O_2 for 24, 12, and 6 days, respectively, in the High Pressure Laboratory at the University of North Dakota. One group, serving as a control, was exposed to a He–O_2 mixture with 200 mm Hg O_2 tension at 1 ATA for 24 days. Compression to 20 ATA was carried out over a 1-hour period with a He–O_2 mixture containing the O_2 tension to be studied. Four animals were removed every 4 days in the two 24-day exposure groups, every 2 days in the 12-day exposure group, and every day in the 6-day exposure group. The animals were decompressed following a 4-hour continuous decompression schedule (Bares 1974).

The animals were fed and watered ad libitum from feeding mechanisms in the chambers. The chambers were cleaned and feeding mechanisms were recharged every 48 hours without altering the environment to which the animals were exposed. During compression and decompression, the pressure levels and time intervals were controlled by an IBM 1800 computer. Throughout the duration of the exposure period, the pressure was controlled by an automatic mechanism. Oxygen concentration was measured every 6 hours and was maintained at the various experimental levels with no more variation than ± 10 mm Hg O_2. Temperature and humidity were controlled at 31.1–33.4°C and 38–44%, respectively. Chamber gases were continuously circulated and filtered through a molecular sieve tower to remove any contaminants before the gas was returned to the chambers.

Following decompression the animals were anesthetized with pentobarbital sodium (35 mg/kg). Lungs removed from three animals per group were lightly blotted, weighed, quick-frozen in liquid nitrogen, and freeze-dried for wet–dry measurements. The lungs of the remaining animal in each group were immediately perfused via the trachea at a hydrostatic pressure of approximately 30 cm of water, with glutaraldehyde-paraformaldehyde buffered at a pH of 7.3 with 0.2 N sodium cacodylate (Karnovsky, 1965).

After the lungs had filled with perfusate, the thoracic cavity was massaged gently to insure total insufflation of the fixative. The lungs were allowed to fix for 2 hours, the thoracic cavity was opened, and the lungs were excised. They were submersed in fixative for an additional 2 hours and then selected tissue specimens were obtained from both superior and inferior positions in the lungs. Specimens prepared for scanning electron microscopy were rinsed in 0.144 N cacodylate buffer postfixed in 2.0% cacodylate buffered OsO_4 for 1 hour, dehydrated in a graded series of acetone, and critical-point dried in a Sorvall Critical Point System, using liquid CO_2. The dried tissues were mounted on specimen stubs with Electrodag, an electrically conductive adhesive, and coated with carbon and palladium-gold in a Denton Vacuum DV 502 high-vacuum evaporator. Specimens were viewed in a Cambridge Stereoscan S4 scanning electron microscope.

RESULTS

Table 1 summarizes the body weights and lung weights obtained from animals exposed to 20 ATA He–O_2 with varying O_2 levels.

TABLE 1
Percent initial body weight—percent lung water and lung dry weight

Exposure group	Exposure Days	Sample size	% Initial body weight Mean ± SD	Sample size	% Lung water Mean ± SD	Lung dry weight Mean ± SD
1 ATA,	4	4	72 ± 1	3	78.5 ± 2.7	0.3607 ± 0.0464
200 mm Hg P_{O_2}	8	3	117 ± 8	2	81.2 ± 0.5	0.5309 ± 0.0190
	12	2	100 ± 1	1	80.9 ± 1.0	0.5036 ± —
	16	4	122 ± 12	3	81.1 ± 0.2	0.5692 ± 0.0486
	20	4	123 ± 4	3	80.2 ± 0.4	0.6041 ± 0.0397
	24	4	109 ± 7	3	80.0 ± 0.1	0.5468 ± 0.0408
20 ATA,	4	4	83 ± 2	3	79.9 ± 0.2	0.7001 ± 0.2334
200 mm Hg P_{O_2}	8	4	97 ± 4	3	79.6 ± 1.0	0.5264 ± 0.0306
	12	3	94 ± 1	2	80.4 ± 0.3	0.6630 ± 0.0156
	16	3	88 ± 2	2	80.4 ± 0.2	0.5994 ± 0.0293
	20	3	82 ± 7	2	81.8 ± 0.3	0.6697 ± 0.0125
	24	2	118 ± 1	1	80.6 ± 1.0	0.7255 ± —
20 ATA,	2	4	85 ± 8	3	79.8 ± 0.3	0.4545 ± 0.0108
400 mm Hg P_{O_2}	4	4	104 ± 6	3	83.4 ± 2.3	0.4951 ± 0.0677
	6	4	97 ± 4	3	81.5 ± 0.2	0.4986 ± 0.1208
	8	4	96 ± 12	3	80.6 ± 0.4	0.6551 ± 0.2755
	10	4	102 ± 7	3	81.3 ± 0.3	0.6405 ± 0.1568
	12	4	96 ± 12	3	81.0 ± 0.2	0.5590 ± 0.0801
20 ATA,	1	4	101 ± 1	3	81.4 ± 0.3	0.4773 ± 0.0225
600 mm Hg P_{O_2}	2	4	90 ± 10	3	80.2 ± 0.7	0.4443 ± 0.1425
	3	4	84 ± 3	3	81.3 ± 0.4	0.5404 ± 0.1074
	4	4	84 ± 3	3	80.8 ± 0.3	0.6091 ± 0.0619
	5	5	75 ± 6	4	81.3 ± 0.5	0.6226 ± 0.1251

Body weights of control animals, 1 ATA He–O_2 with 200 mm Hg P_{O_2}, showed a progressive increase to over 120% of their original value at 20 days. Lung dry weights followed a similar pattern, increasing from 0.36 to 0.55 g. Lung and body weights of animals exposed to 20 ATA He–O_2 with 200 mm Hg P_{O_2} for 24 days were extremely variable with no definite trend observed. Body weights of animals exposed to 20 ATA He–O_2 with 400 mm Hg P_{O_2} did not increase as the controls' did, but fluctuated around the 100% level. However, the lung dry weight rose slightly over the 12-day exposure. With exposure to 20 ATA He–O_2 with 600 mm P_{O_2}, body weights showed a very definite downward trend. Starting at 101% after 24 hours of exposure, the body weight declined on succeeding days in an almost linear fashion to 75% of its original value on the fifth and last day of exposure. Lung dry weight showed just the opposite pattern, increasing from 0.48 g on the first day to 0.62 g on the fifth day.

In all of the exposure groups, the lung water remained surprisingly constant, at or near 80%.

At the end of the air-conducting system and the beginning of the gas-exchange system is the junction between the terminal bronchiole and respiratory duct (Fig. 1). The airways are surrounded by lung tissue comprised of a complex network of pulmonary vasculature, terminal airways, and alveoli. Attention will be focused on the alveoli momentarily.

The surface of the terminal bronchiole is covered by mucous cells bordered by cilia (Fig. 2). The mucous cells typically have a white mucous cap (Fig. 3). Those mucous cells not bordered by cilia have ridges or microplicae denoting cell boundaries.

The surface epithelium makes an abrupt change at the origins of the respiratory ducts (Fig. 4). The respiratory ducts are characterized in part by the first appearance of alveoli in the

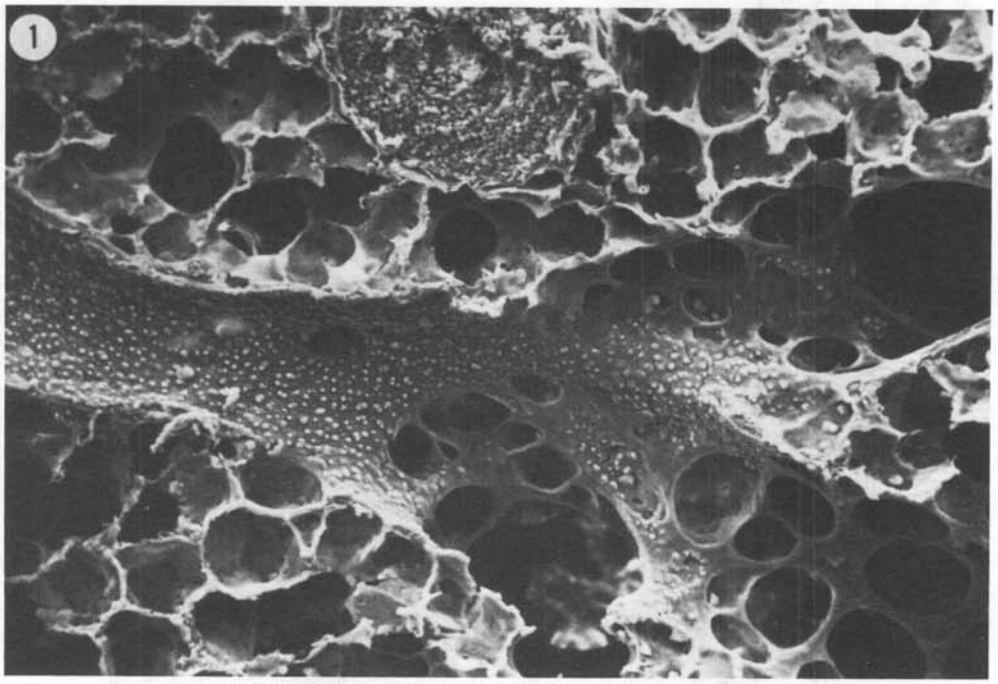

Fig. 1. *Scanning micrograph of terminal bronchiole.* Shown is the junction of a terminal bronchiole with three respiratory ducts. The airway is surrounded by lung tissue comprised of a complex network of pulmonary vasculature, terminal airways, and alveoli. Original magnification 140×. (Photo reduced by 81%)

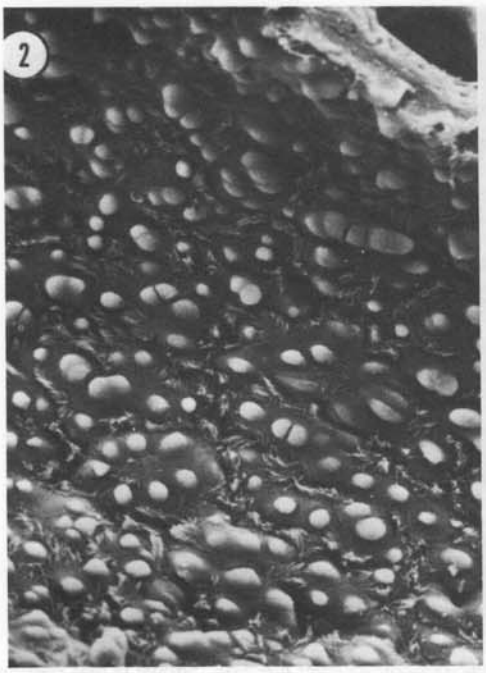

Fig. 2. *Scanning micrograph of mucous cells of the terminal bronchiole*. Original magnification 630×. (Photo reduced by 81%)

Fig. 3. *Scanning micrograph of cilia border of mucous cells*. Those cells not bordered by cilia can be shown to have microplicae denoting their cell boundaries, as in the lower left corner of this micrograph. Original magnification 2100×. (Photo reduced by 81%)

airway. In the respiratory duct, there is an immediate and total loss of mucous cells and cilia, which were quite prominent in the terminal bronchiole. The respiratory-duct epithelium now takes on the characteristics of simple squamous cells. The basis for considering the respiratory duct part of the gas-exchange system is very apparent. Readily discernible are erythrocytes lying within the capillaries of the alveolar-capillary system (Fig. 5).

Figures 6 through 9 are micrographs of alveoli which are morphologically very similar and are typical of normal alveoli even though their exposures differ. Figure 6 is a scanning electron micrograph showing one alveolus and part of a second which have been exposed to 1 ATA $He–O_2$ with 200 mm Hg P_{O_2} for 4 days. The alveolus is covered by a smooth-surfaced epithelium interrupted by numerous Kohns pores. In the top center and lower left can be seen two rough-surfaced alveolar type-II cells. The alveolar type-II cell's surface is made up of numerous short and somewhat rounded microvilli (Fig. 7). Cell boundaries of alveolar type-I cells can be distinguished by microplicae or small ridges at cell junctions. Also evident in Fig. 7 is a Kohns pore through which an adjacent alveolus can be seen.

Alveoli exposed to 20 ATA $He–O_2$ with 200 mm Hg P_{O_2} for 4 days appear very similar to the 1-ATA exposed alveoli (Fig. 8). The alveolus appears to be cup-shaped with very thin, delicate sepata separating it from other alveoli. The epithelium is smooth and contains several pores. At left center of Fig. 8 is an alveolar type-II cell which can be seen in Fig. 9. In the upper right corner of Fig. 8 are two alveolar type-II cells in adjacent alveoli. Figure 9 shows a typical alveolar type-II cell with short, rounded microvilli covering its surface. In the center of the cell

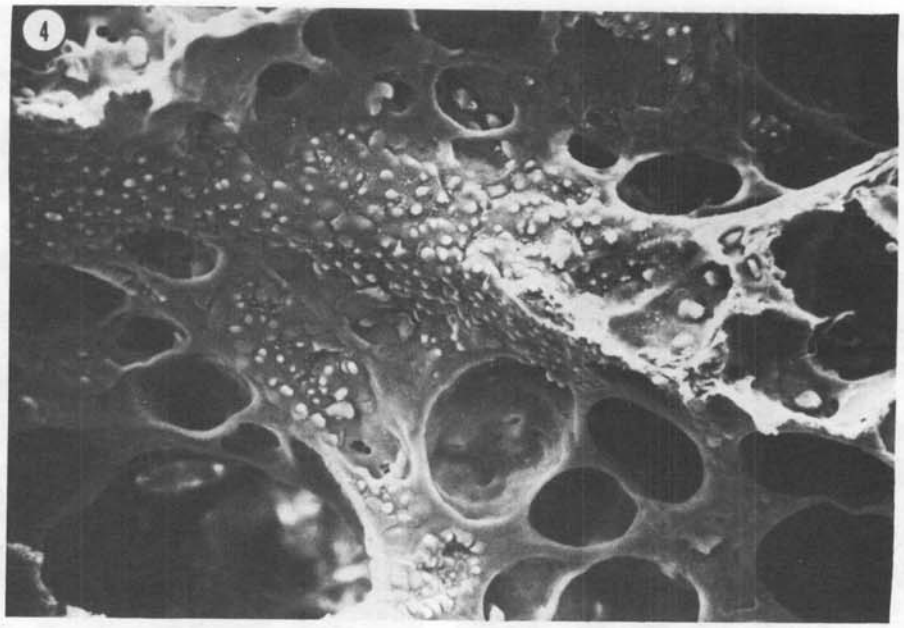

Fig. 4. *Scanning micrograph of terminal bronchiole–respiratory duct junction.* Shown is that portion of Fig. 1 at which the airway epithelium abruptly changes from mucous cells bordered by cilia, characteristic of the terminal bronchiole, to the simple squamous epithelium of the respiratory duct. Also evident is the first appearance of alveoli. Original magnification 210×. (Photo reduced by 85%)

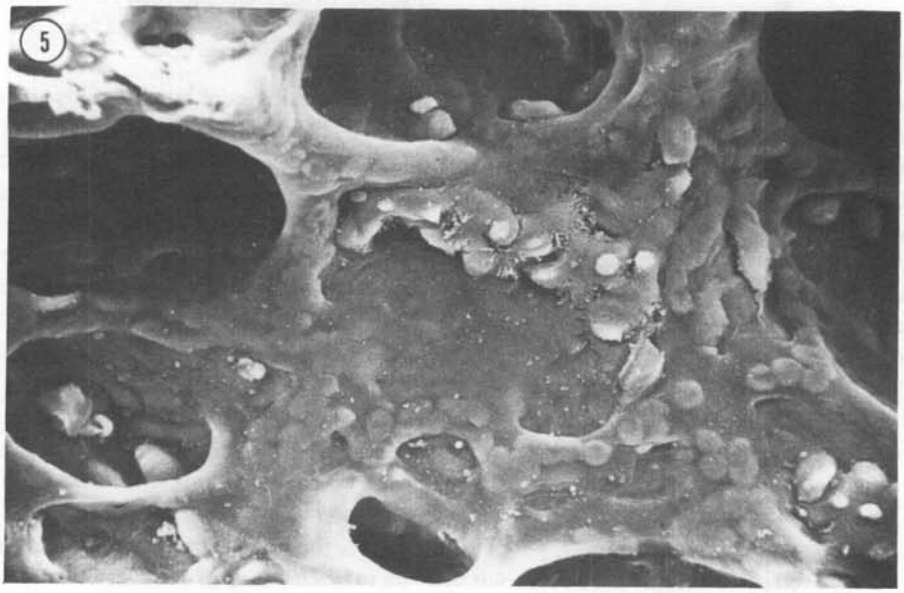

Fig. 5. *Scanning micrograph of respiratory duct.* Shown are the last few mucous cells (considered by some to be Clara cells) of the terminal bronchiole with their bordering cilia. Very apparent are the erythrocytes outlined within the capillaries under the very delicate epithelium now present. Original magnification 650×. (Photo reduced by 85%)

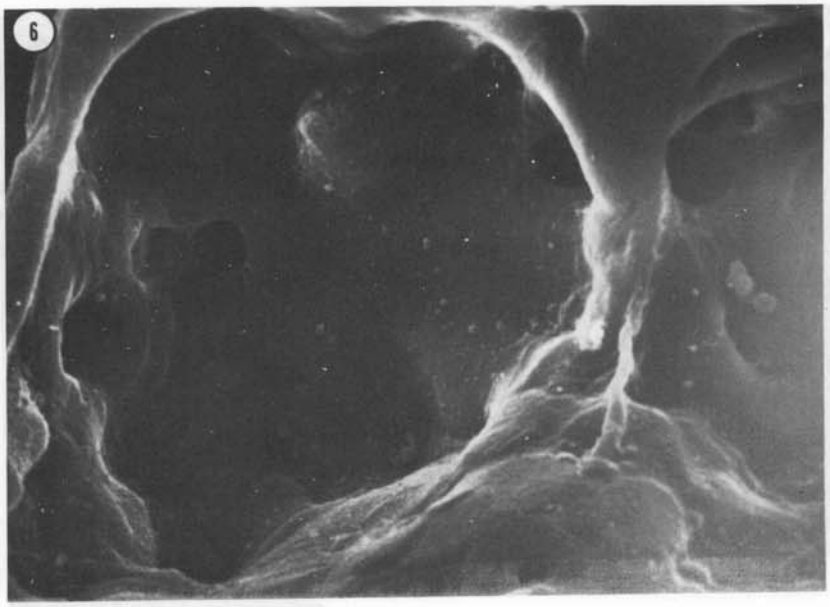

Fig. 6. *Scanning micrograph of alveolus exposed to 1 ATA He–O_2 with 200 mm Hg P_{O_2} for 4 days.* Shown is a typical alveolus with its smooth-surfaced epithelium. The alveolar surface is interrupted by numerous pores (Kohns), which allows communication between alveoli. In top center and lower left can be seen two rough-surfaced alveolar type-II cells. Original magnification 2800×. (Photo reduced by 80%)

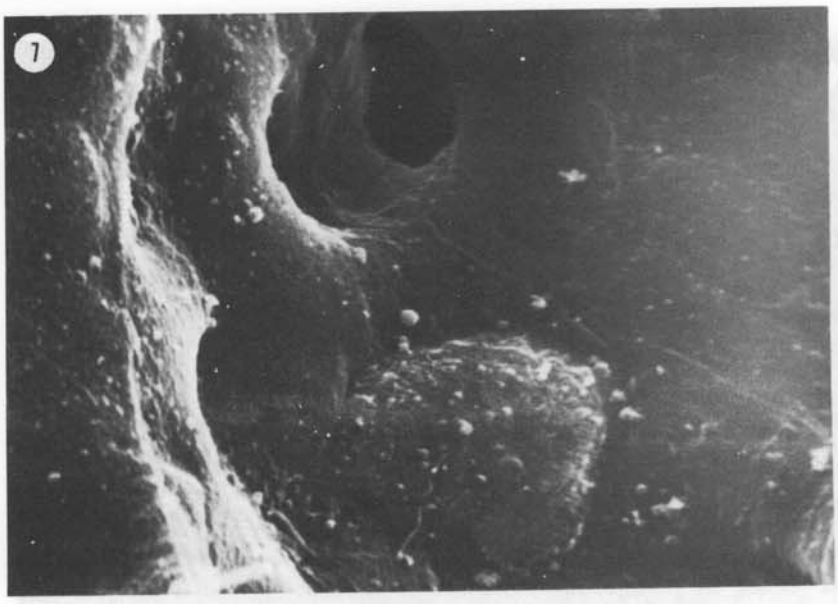

Fig. 7. *Scanning micrograph of alveolar type-II cell exposed to 1 ATA He–O_2 with 200 mm Hg P_{O_2} for 4 days.* Shown is the rough-surfaced, microvilli-covered, alveolar type-II cell. The microvilli appear to be short and somewhat rounded. Also shown is a Kohns pore through which the adjacent alveolus can be seen. Cell boundaries of alveolar type-I cells can be distinguished by microplicae elevations at cell junctions. Original magnification 3900×. (Photo reduced by 80%)

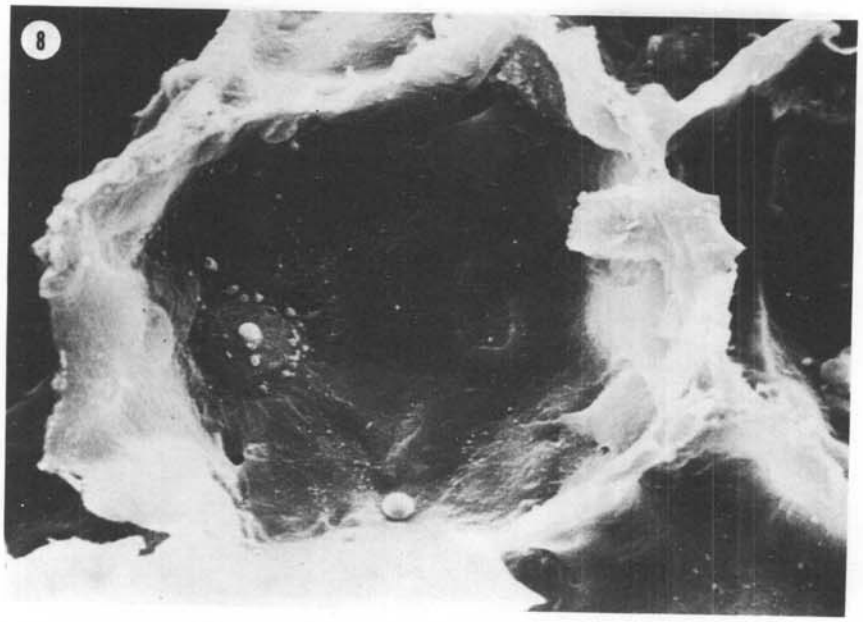

Fig. 8. *Scanning micrograph of alveolus exposed to 20 ATA He–O_2 with 200 mm Hg P_{O_2} for 4 days.* Shown is a normal alveolus with typical smooth-surface appearance. At left center is an alveolar type-II cell seen in Fig. 9. Also shown are a number of small Kohns pores. Original magnification 1700×. (Photo reduced by 81%)

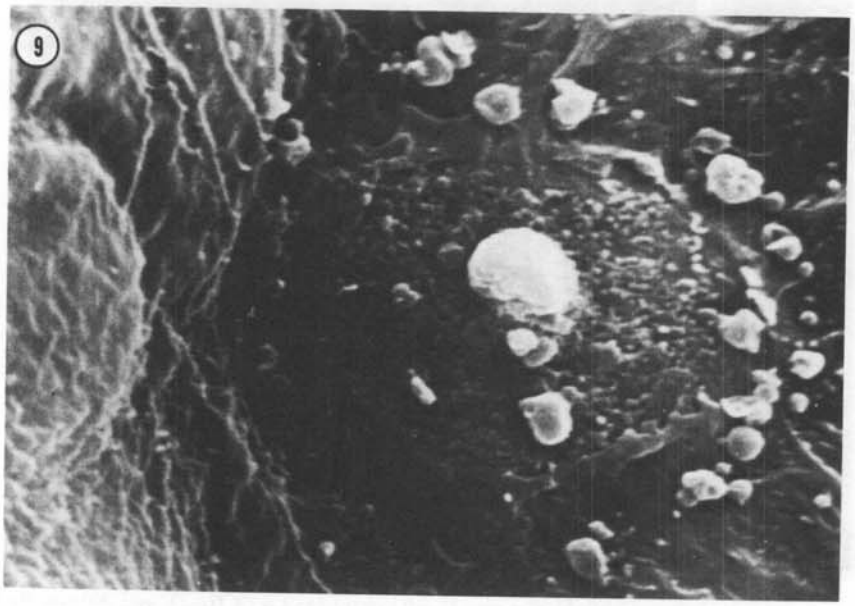

Fig. 9. *Scanning micrograph of alveolar type-II cell exposed to 20 ATA He–O_2 with 200 mm Hg P_{O_2} for 4 days.* Shown is a typical alveolar type-II cell, the surface of which is covered by numerous small microvilli. In the center of the cell is what appears to be a mass of material (surfactant) being secreted from the cell. Original magnification 17,600×. (Photo reduced by 81%)

is what appears to be a mass of material being secreted from the cell. Alveolar free-cells or macrophages were seldom seen in the alveoli.

Figure 10 shows a group of alveoli exposed to 1 ATA He–O_2 with 200 mm Hg P_{O_2} for 24 days. Readily apparent are the erythrocytes in the capillary network. The alveolar septae do not appear thickened. However, there is an obvious increase in the number of macrophages in the alveoli (top center and lower right). The Kohns pores are still patent and the alveolar type-II cells show no apparent change.

Alveoli exposed to 21 ATA He–O_2 with 200 mm Hg P_{O_2} for 24 days have an appearance similar to those exposed to 1 ATA for the same length of time (Fig. 11). The alveolar walls and Kohns pores appear unaltered. Again, erythrocytes are observable in the capillary network under the alveolar epithelium.

After 12 days exposure to 21 ATA He–O_2 with 400 mm Hg P_{O_2}, few overt changes in the alveoli can be observed (Fig. 12). The alveolar septae do not appear thickened and erythrocytes can be observed under the alveolar epithelium. However, there appears to be an increased macrophagic infiltration into many of the alveoli, as in the left center of Fig. 12. An even more subtle change can be observed when the area immediately under the macrophages in Fig. 12 is scanned at greater magnification (Fig. 13). Figure 13 shows an alveolar type-II cell partially covered by a macrophage. Of particular importance in this micrograph is the tremendous increase in length of the microvilli covering the surface of the cell.

Alveoli exposed to 20 ATA He–O_2 with 600 mm Hg P_{O_2} for 1 day show very few overt changes (Fig. 14). The alveolar epithelium is smooth and undamaged. Erythrocytes are still readily seen under the epithelium. A macrophage is seen in the lower-right portion of the alveolus. The alveolar type-II cell, with a pseudopodic extension across the alveolar surface, looks very much intact. However, some of the alveolar type-II cells show a lengthening of the microvilli covering their surfaces (Fig. 15).

After 5 days exposure to 20 ATA, 600 mm Hg P_{O_2}, some of the alveoli still appear undamaged (Fig. 16). Macrophages are more prevalent. The alveoli without macrophages are the exception, not the rule. Careful examination of the epithelial surface in Fig. 16 shows an increased population of alveolar type-II cells, as indicated by the arrows.

Many of the alveoli in the 5-day exposed lungs appear to be coated with a layer of material which completely obscures the Kohns pores and surfaces of the alveolar type-II cells (Fig. 17).

The majority of the lung tissue after 5 days of hyperbaric exposure with 600 mm Hg P_{O_2} has tremendous macrophagic infiltration (Figs. 18 and 19). The macrophages appear to be surrounded by a fibrin-like matrix (Fig. 18). Many of the alveolar septae show total disruption. If the alveolar type-II cells are present, they are totally obscured. The disruption has progressed to such a degree that much of the specimen appears as an amorphous mass of lung tissue.

DISCUSSION

The functional unit of the lung concerned with O_2 transport is the alveolus. Oxygen transport is maintained only as long as the very delicate structure of the alveolus remains intact. Of particular structural importance is the alveolar surface, which is the first structure which gases encounter and through which they must pass to enter the circulating blood. Thus, any pathological condition—such as O_2 toxicity—that alters the alveolar surface must also alter pulmonary function.

Pulmonary O_2 toxicity is a progressive disease which develops when the P_{O_2} in inspired air rises to between 0.75 and 2.0 atm (Clark and Lambertsen 1971). The most generally recog-

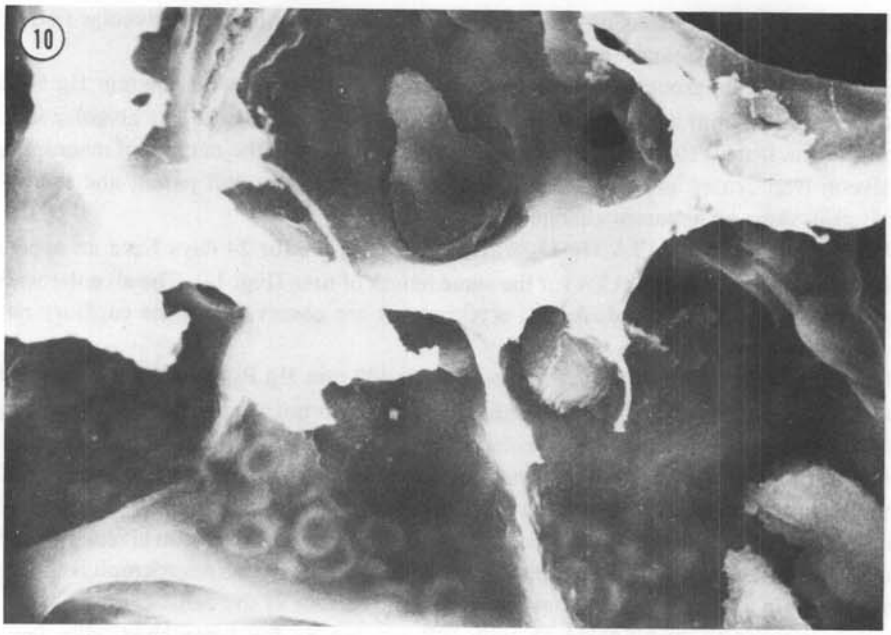

Fig. 10. *Scanning micrograph of alveolus exposed to 1 ATA He–O_2 with 200 mm Hg P_{O_2} for 24 days.* Erythrocytes can readily be seen underlying the alveolar epithelium. Kohns pores are still patent. An increased number of macrophages can be seen in the alveoli. Original magnification 1400×. (Photo reduced by 87%)

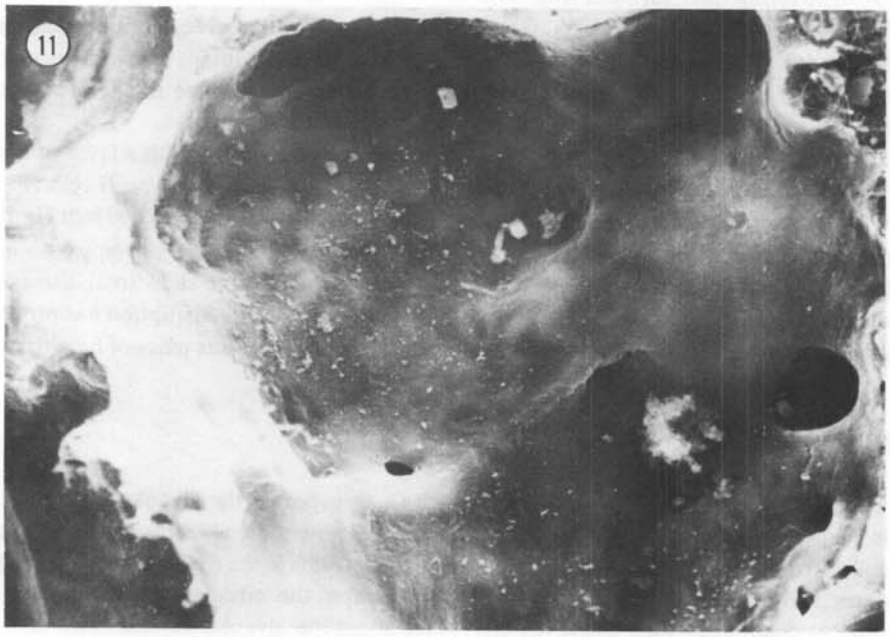

Fig. 11. *Scanning micrograph of alveolus exposed to 20 ATA He–O_2 with 200 mm Hg P_{O_2} for 24 days.* Alveolar epithelium can be seen, still intact. Erythrocytes are outlined within the alveolar capillaries and the Kohns pores are still patent. Original magnification 2800×. (Photo reduced by 87%)

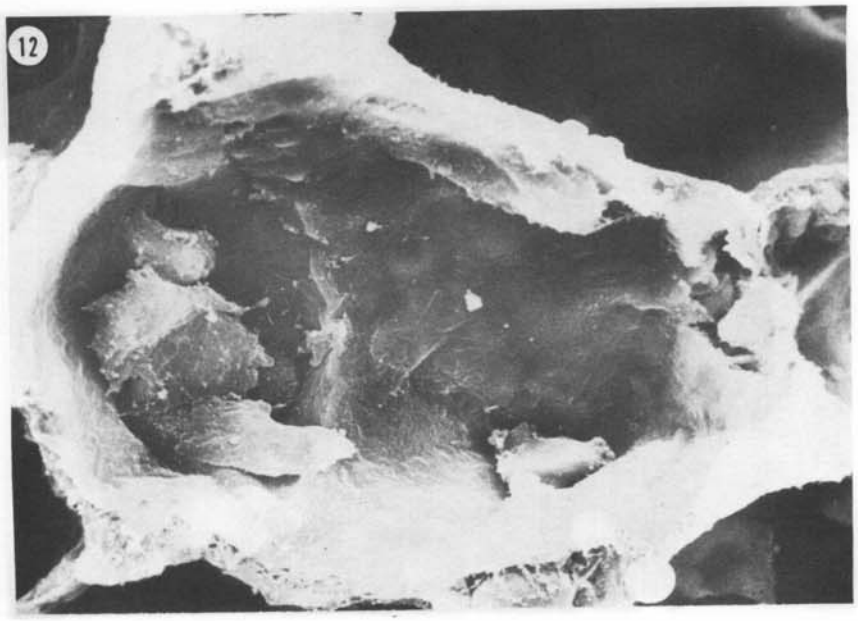

Fig. 12. *Scanning micrograph of alveolus exposed to 20 ATA He–O_2 with 400 mm Hg P_{O_2} for 12 days.* Shown are a number of alveolar macrophages (left center) covering an alveolar type-II cell, which can be seen in Fig. 13. Still evident are erythrocytes underlying the alveolar epithelium. Original magnification 1500×. (Photo reduced by 81%)

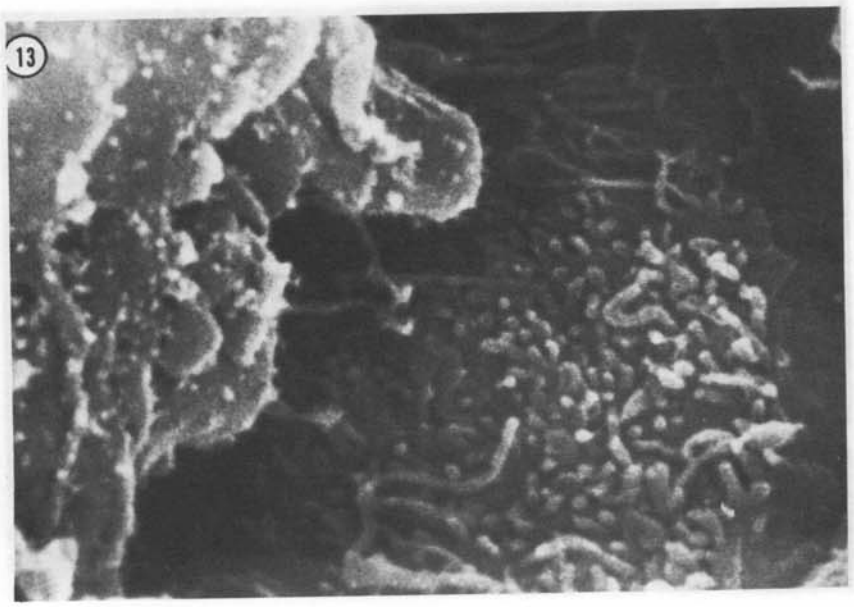

Fig. 13. *Scanning micrograph of alveolar type-II cell exposed to 20 ATA He–O_2 with 400 mm Hg P_{O_2} for 12 days.* Shown is an alveolar type-II cell partially covered by an alveolar macrophage. Although many of the microvilli appear small and round, some of them have increased in length significantly. Original magnification 18,460×. (Photo reduced by 81%)

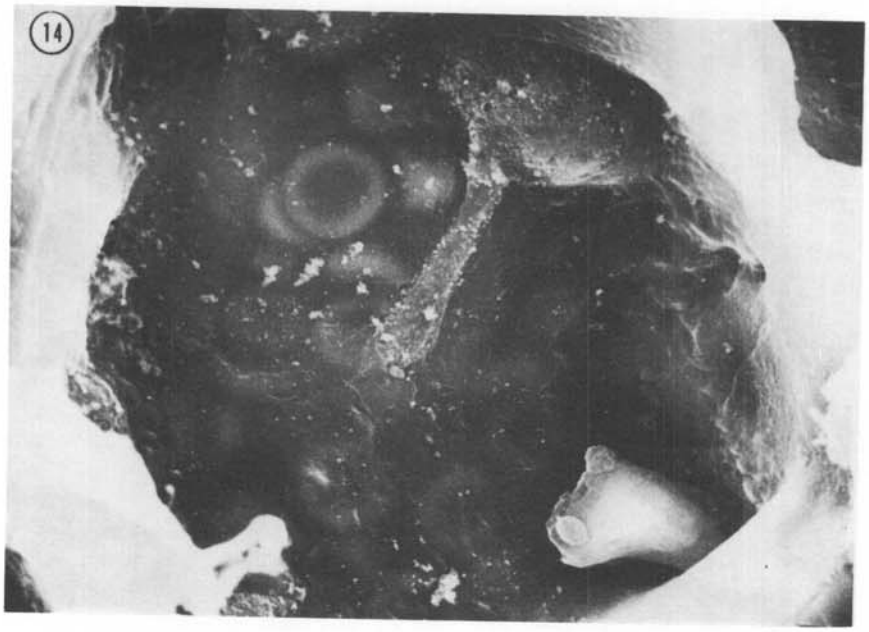

Fig. 14. *Scanning micrograph of alveolus exposed to 20 ATA He–O_2 with 600 mm Hg P_{O_2} for 1 day.* Erythrocytes are very apparent under the alveolar epithelium. At upper right is an alveolar type-II cell with a pseudopodic extension. In lower right corner of alveolus is an alveolar macrophage. Original magnification 2700×. (Photo reduced by 85%)

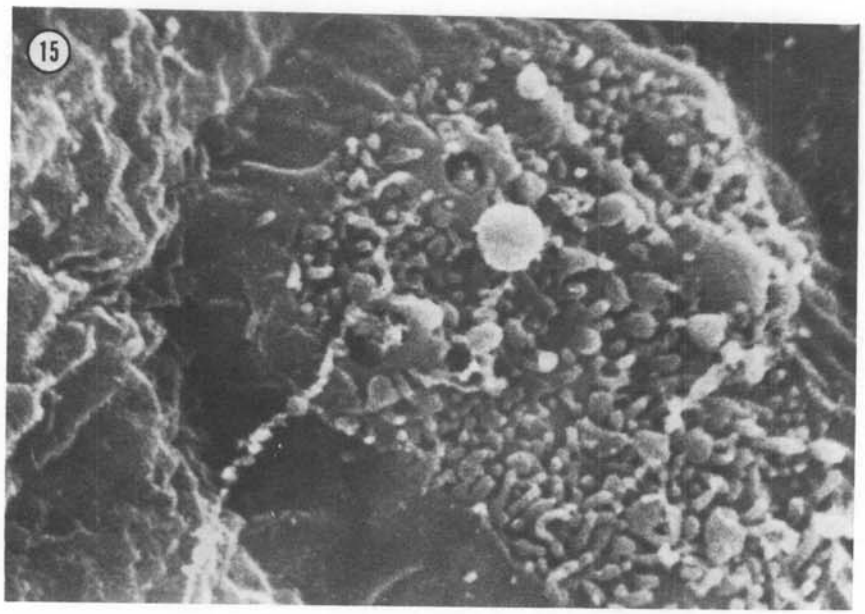

Fig. 15. *Scanning micrograph of alveolar type-II cell exposed to 20 ATA He–O_2 with 600 mm Hg P_{O_2} for 1 day.* Many of the microvilli covering the surface of the alveolar type-II cell are elongated. At upper center is a small pit which may be an area where cellular material has recently been secreted. Original magnification 15,390×. (Photo reduced by 85%)

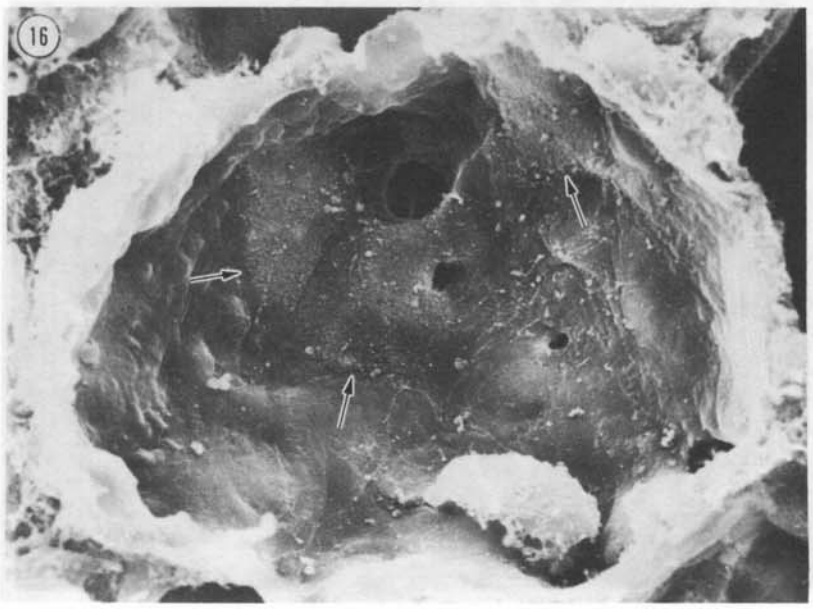

Fig. 16. *Scanning micrograph of alveolus exposed to 20 ATA He–O_2 with 600 mm Hg P_{O_2} for 5 days.* Shown is an alveolus with increased population of alveolar type-II cells (indicated by arrows). Also shown in lower right is an alveolar macrophage. The Kohns pores still appear patent. Original magnification 2900×. (Photo reduced by 81%)

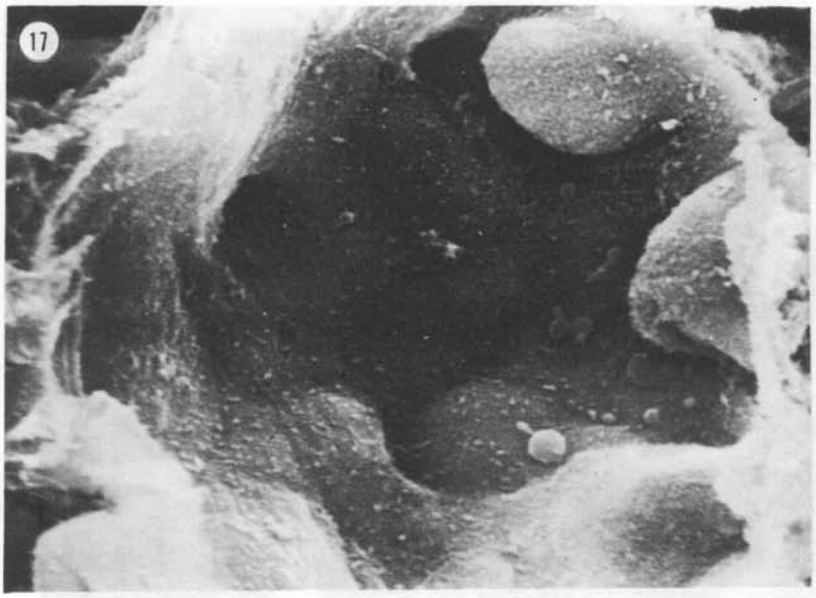

Fig. 17. *Scanning micrograph of coated alveolus exposed to 20 ATA He–O_2 with 600 mm Hg P_{O_2} for 5 days.* The alveolus appears coated by a layering of material which completely obscures the Kohns pores and covers the surfaces of the alveolar type-II cells. Original magnification 2300×. (Photo reduced by 81%)

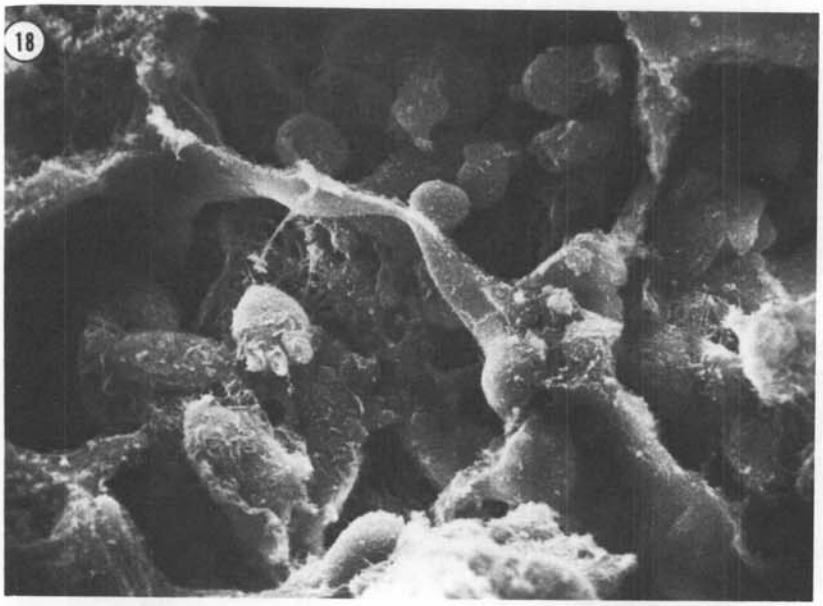

Fig. 18. *Scanning micrograph of 5-day toxic lung with fibrin mat and macrophagic involvement.* Shown are three severely oxygen-toxic alveoli with significant macrophagic infiltration. Also shown is what appears to be a fibrin-like matrix surrounding many of the macrophages. The alveolar walls appear to have lost their integrity in some areas. The lungs were exposed to 20 ATA He–O_2 with 600 mm Hg P_{O_2} for 5 days. Original magnification 1500×. (Photo reduced by 80%).

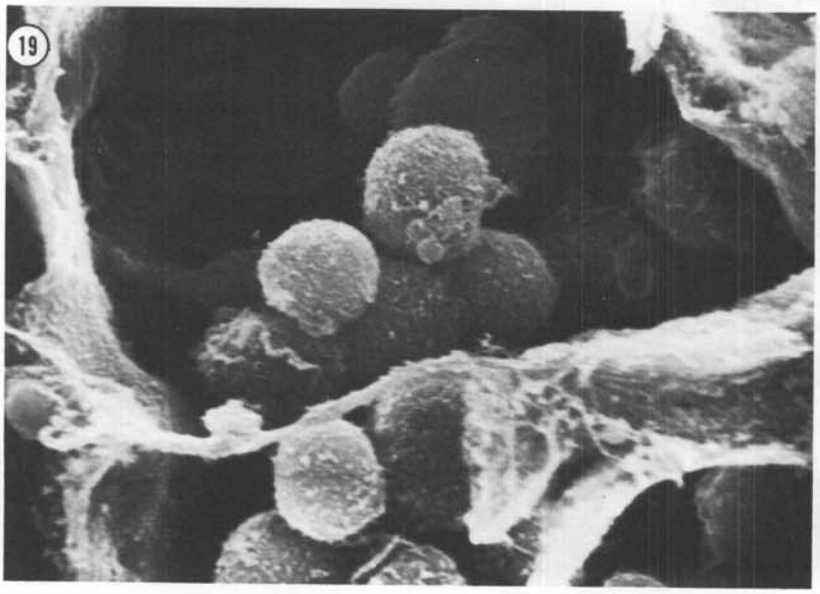

Fig. 19. *Scanning micrograph of 5-day toxic lung with macrophagic involvement.* Shown are portions of two alveoli from animals exposed to 20 ATA He–O_2 with 600 mm Hg P_{O_2} for 5 days. Numerous macrophages can be seen infiltrated into the alveoli. Original magnification 2320×. (Photo reduced by 80%)

nized course followed in O_2 toxicity includes: pulmonary damage interfering with the diffusion of respiratory gases across the respiratory membranes; hypoxemia; and, finally, acidosis terminating in death of the animal (Kaplan, Robinson, Kapanci, and Weibel 1969; Robinson, Sopher, and Witchett 1969). The pathologies most commonly seen are edema, atelectasis, fibrin formation, alveolar cell hypertrophy, arteriolar thickening, desquamation, and tissue degeneration (Bean 1945; Clark and Lambertsen 1971).

In this study, few conclusions can be drawn using tissue-weight analysis. The only series of animals for which there is even indirect evidence of the occurrence of pulmonary O_2 toxicity is the 600 mm Hg P_{O_2} series. This group showed a fall in body weight with an increase in lung dry weights. A slight increase in lung dry weight was also seen in the last days of exposure to 400 mm Hg P_{O_2}. This can be explained after studying the electron micrographs taken of lung specimens from these animals. The lung water did not increase in any of the exposure groups, indicating the absence of large amounts of fluids accumulating in the lung tissue. The failure to demonstrate significant alterations in tissue weights upon exposure to increased O_2 concentrations does not preclude the possibility of subtle morphological changes, detectable only by ultrastructural microscopic examination.

After 24 days exposure to He–O_2 with 200 mm Hg P_{O_2} at both 1 and 20 ATA, there was no apparent damage to the alveolar morphology. The alveolar type-I and -II cells appeared undamaged. The Kohns pores remained patent. The interstitial spaces did not appear thickened, which was evidenced by the fact that erythrocytes in the alveolar-capillary network were readily discernible beneath the alveolar epithelium. However, there was one noticeable change. Alveolar free-cells, or macrophages, were much more numerous in animals after prolonged exposure to He–O_2. This did not appear to be an effect of pressure since animals exposed to both 1 ATA and 20 ATA showed similar increases in macrophagic populations.

Animals exposed to an increased O_2 concentration, 400 mm Hg P_{O_2}, for 12 days also showed very little overt damage. There was an increased macrophage population in the alveoli similar to that of the 24-day exposure; however, this increase was noticeable after only 12 days of exposure. A less noticeable but even more important change occurred in the alveolar type-II cell. The microvilli covering the type-II cell surface appeared greatly lengthened.

Changes in the appearance and number of cell microvilli have been shown to occur during the various stages in the cell cycle (Porter, Prescott, and Frye 1973) and in response to alterations in the physiological environment to which the cell is exposed, such as changes in tonicity (Peine and Low 1975) or changes in pH. These changes have been shown to occur after as little as 5 min of exposure to the altered environment. Numerous alterations in alveolar type-II cells have been reported in previous pulmonary O_2 toxicity studies but none have mentioned microvilli changes. However, transmission and light micrographs would not have allowed such conclusions to be drawn unless very careful serial sections had been done on the specimens. As can be seen from the scanning micrographs, the lengthened microvilli do not stand straight up but rather lie on the surface of the cell and thus in a normal section could be mistaken for a typical microvilli.

Exposure to 600 mm Hg P_{O_2} at 20 ATA resulted in even greater macrophagic involvement. After only 1 day of exposure, macrophages could be found easily in the alveoli. The alveolar wall does not appear thickened, however, inasmuch as erythrocytes are still very apparent under the alveolar epithelium. An indication of even more serious damage is the elongation of the type-II microvilli, which is already evident at 1 day. After 5 days there was a tremendous infiltration of macrophages into most of the alveoli. The increased population of macrophages in both the 400- and 600-mm Hg O_2 groups could be responsible for much of the increase in dry weight of the lung. Cohn Hirsch, and Fedorko (1966) found that stimulation of macrophage production resulted in a change in macrophage cell size and an increase in cellular dry mass.

The macrophages were seen to be surrounded by a matrix of fibrin-like material. Intra-alveolar fibrin is not an uncommon finding in the O_2-toxic lung (Adamson et al. 1970; Cedergren et al. 1959; Bruns and Shields 1954). In those alveoli which appear relatively normal after 5 days exposure to 600 mm Hg P_{O_2}, an increased population of alveolar type-II cells was found to occur. This has been reported previously in transmission electron microscopy (Kapanci et al. 1969; Schaffner, Felig, and Trachtenberg 1967). Much of the lung specimen from the severely toxic lung appeared as an amorphous mass of tissue with complete disruption of the alveolar walls.

Many of the observations reported in this study have been reported by earlier light and electron microscopic studies. However, the importance of this study lies in the fact that this was one of the first studies to allow near three-dimensional visualization of many of the morphological alterations which occur during the development of O_2 toxicity. It has also shed light on some very early but subtle pulmonary changes that occur before O_2 toxicity becomes clearly symptomatic. This may necessitate the reevaluation of the lower O_2 limit ascribed to be responsible for the development of pulmonary O_2 toxicity.

This study was supported in part by Contract No. N00014-68-A-0499 [NR 101-753], between the Office of Naval Research, U.S. Department of the Navy, and the University of North Dakota. It was also supported by NIH Training Grant 1 T01 HL05939-01A1. The scanning electron microscope used in this study was purchased on NIH Grant No. NS 09363.—*Received for publication October 1975; revised manuscript received July 1976.*

Ross, B.K., and T.K. Akers. 1976. Microscopie électronique à balayage de poumons exposés à l'hyperbarie normoxique et hyperoxique. Undersea Biomed. Res. (3):283–299.—Des poumons de cobayes adultes exposés à 1 ATA de He–O_2 (200 mm Hg P_{O_2}) et à 20 ATA He–O_2 (200, 400, et 600 mm Hg P_{O_2}) ont été étudiés par microscopie électronique à balayage. Les alvéoles normaux sont décrits. Même avant l'apparition des symptomes de toxicité de l'oxygène, des altérations discrètes sont remarquées dans les alvéoles, surtout un nombre accrue de macrophages et une longeur accentuée des microvilli cellulaires alvéolaires type II. Ces altérations ont été notées chez des animaux exposés à 400 mm Hg P_{O_2}, considéré jusqu'à présent en dessous des niveaux toxiques. Avec une toxicité accrue, le nombre de cellules alvéolaries type II a augmenté. Une couche épaisse est notée dans certains alvéoles, cachent les pores de Kohn et les surfaces cellulaires types I et II. Le reseau alvéolaire-capillaire avec ses érythrocytes n'était plus visible. Dans les poumons les plus exposés sont remarqués de grandes quantités de macrophages dans une matrice qui ressemble au fibrine. Les parois alvéolaires étaient souvent détruits, et les alvéoles n'étaient plus des entités particulaires, mais plutot une masse amorphe de tissu pulmonaire.

toxicité de l'oxygène
alvéole
macrophage
cellules alvéolaries type II

REFERENCES

Adamson, I.Y.R., D.H. Bowden, and J.P. Wyatt. 1970. Oxygen poisoning in mice. Ultrastructural and surfactant studies during exposure and recovery. Arch. Pathol. 90: 463–472.

Aranyi, C. 1972. Effect of cigarette smoke on the surface morphology of rabbit alveolar macrophages as observed by scanning electron microscopy. J. Cell Biol. 55(2): 5a.

Bares, W.A. 1974. Optimum diving profiles. Bulletin Number 74307, Instrument Society of America, Pittsburgh, Pa. pp. 29–32.

Bean, J.W. 1945. Effects of oxygen at high pressure: a review. Physiol. Rev. 25: 1–147.

Bruns, P.D., and L.V. Shields. 1954. High O_2 and hyaline-like membranes. Am. J. Obstet. Gynecol. 67: 1224–1236.

Cedergren, B., L. Gyllensten, and J. Wersall. 1959. Pulmonary damage caused by oxygen poisoning: electron microscopic study in mice. Acta Paediatr. Scand. 48: 477–494.

Clark, J.M., and C.J. Lambertsen. 1971. Pulmonary oxygen toxicity: a review. Pharmacol. Rev. 23: 37–133.

Cohn, Z.A., J.G. Hirsch, and M.E. Fedorko. 1966. The in vitro differentiation of mononuclear phagocytes. IV. The ultrastructure of macrophage differentiation in the peritoneal cavity and in culture. J. Exp. Med. 123: 747–757.

Greenwood, M.F., and P. Holland. 1972. The mammalian respiratory tract surface: a scanning electron microscopic study. Lab. Invest. 27: 296–304.

Greenwood, M.F., and P. Holland. 1973. Scanning electron microscopy of the normal and BCG-stimulated primate respiratory tract. J. Reticulo-endothel. Soc. 13: 183–192.

Holma, B. 1969. Scanning electron microscopic observations of particles deposited in the lung. Arch. Environ. Health 18: 330–339.

Jaques, W.E., J. Coalson, and A. Zervins. 1965. Application of the scanning electron microscope to human tissues. A preliminary study. Exp. Mol. Pathol. 4: 576–580.

Kapanci, Y., E.R. Weibel, H.P. Kaplan, and F.R. Robinson. 1969. Pathogenesis and reversibility of pulmonary lesions of oxygen toxicity in monkeys. II. Ultrastructural and morphometric studies. Lab. Invest. 20: 101–118.

Kaplan, H.P., F.R. Robinson, Y. Kapanci, and E.R. Weibel. 1969. Pathogenesis and reversibility of pulomonary lesions of oxygen toxicity in monkeys. I. Clinical and light microscopic studies. Lab. Invest. 20: 94–100.

Karnovsky, M.J. 1965. Formaldehyde–glutaraldehyde fixative of high osmolarity for use in electron microscopy. J. Cell. Biol. 27: 137A.

Kistler, G.S., P.R.B. Caldwell, and E.R. Weibel. 1967. Development of fine structural damage to alveolar and capillary lining cells in oxygen-poisoned rat lungs. J. Cell Biol. 32: 605–628.

Kuhn, C., and E.H. Finke. 1972. The topography of the pulmonary alveolus: scanning electron microscopy using different fixations. J. Ultrastruct. Res. 38: 161–173.

Nowell, J.A., and W.S. Tyler. 1971. Scanning electron microscopy of the surface morphology of mammalian lungs. Am. Rev. Respir. Dis. 103: 313–328.

Peine, C.J., and F.N. Low. 1975. Scanning electron microscopy of cardiac endothelium of the dog. Am. J. Anat. 142: 137–158.

Porter, K., D. Prescott, and J. Frye. 1973. Changes in surface morphology of Chinese hamster ovary cells during the cell cycle. J. Cell Biol. 57: 815–836.

Robinson, F.R., R.L. Sopher, and C.E. Witchett. 1969. Pathology of normobaric oxygen toxicity in primates. Aerosp. Med. 40: 879–884.

Schaffner, F., P. Felig, and E. Trachtenberg. 1967. Structure of rat lung after protracted oxygen breathing. Arch. Pathol. 83: 99–107.

Wang, N., and W.M. Thurlbeck. 1970. Scanning microscopy of the lung. Hum. Pathol. 1: 227–231.